



# Selenology Today

11203/ 16:48:53 UT

© George Tarsoulis (Democritus Observatory) - www.lunar-captures.com

**Selenology Today 26      January 2012**



# Selenology Today Issue 26 January 2012

*Selenology Today is devoted to the publication of contributions in the field of lunar studies. Manuscripts reporting the results of new research concerning the astronomy, geology, physics, chemistry and other scientific aspects of Earth's Moon are welcome. Selenology Today publishes papers devoted exclusively to the Moon. Reviews, historical papers and manuscripts describing observing or spacecraft instrumentation are considered.*

*The Selenology Today Editorial Office: [selenology\\_today@christian-woehler.de](mailto:selenology_today@christian-woehler.de)*

**Kurt A. Fisher: New Developments in Counting Very Small Lunar Craters .....1**

**George Tarsoudis: An unnamed feature like a fault termed "Piccolomini-Brenner" .....25**

**Raffaello Lena and Jim Phillips: Lunar Domes near Gambart C.....31**



**Editor-in-Chief:**  
**R. Lena**

**Editors:**  
**M.T. Bregante**  
**J. Phillips**  
**C. Wöhler**  
**C. Wood**

**Selenology Today website**  
<http://digilander.libero.it/glrgroup/>

**Cover George Tarsoudis**



**Kurt A. Fisher: New Developments in Counting Very Small Lunar Craters**

## **New Developments in Counting Very Small Lunar Craters**

by Kurt A. Fisher

### **Abstract**

*Controversies regarding the validity of lunar crater production curves from small lunar crater counting cannot be fully resolved without improved Crater Detection Algorithm (CDA) software. The counting accuracy of current CDA software is low, and development of improved software requires matched sets of Lunar Reconnaissance Orbiter Narrow Angle Camera (NAC) images taken under both high and low solar illumination. For future work, we propose to prepare two cross-reference indices from the 503,206 LRO images published by the LROC Team through Release No. 7 in Sept. 2011: first, where Lunar Orbiter V (LOV) high resolution high solar illumination images overlap NAC low-illumination images, and second, where high and low solar illumination NAC images of nearside lunar mares overlap, if any. A follow up article will illustrate the use of NASA PDS View to extract subparts from NAC images and how to locate candidate NAC images using the LRO Image Browser and ACT-REACT Map.*

### **1. Introduction**

Xiao & Strom's recent finding questioning the validity of small lunar crater counts ( $100\text{m} \geq D < 1\text{km}$ ) should be deferred for very small craters ( $5\text{m} \geq D < 100\text{m}$ ) until more NAC high solar illumination images can be identified that match existing Lunar Reconnaissance Orbiter (LRO) Narrow Angle Camera (NAC) low solar illumination images. A larger set of NAC overlap images is needed in order to have a statistically valid large sample of very small craters (Xiao & Strom, 2011). The sun incidence variation in crater counts recently re-confirmed by Ostrach et al. (2011) can be controlled for by image selection and computation. Traditional objections to very small crater counting based on secondary impact contamination can be ignored because below the equilibrium saturation point, very small craters are constantly gardened on relatively short time frames, and thus useful spatial frequency diagram (SFD) information may exist under Neukum et al.'s SFD slope for very small craters below saturation equilibrium. Crater production curves based on very small lunar crater counts also might provide an upper boundary constraint on estimates of the lunar meteor impact flux based on real time telescopic monitoring. However, improved accuracy crater detection algorithm (CDA) software is needed in order to resolve these questions, where the best of current CDAs detect between 33% to 83% of craters in an image (Bandeira et al., 2010; Lončarić et al., 2011).

Producing improved CDA software that would automatically count very small craters requires matched NAC high and low solar illumination images that can identify very small craters that are both bright-rayed and that have sharp rims (see illustrative examples Figs 1 through 6). Between 2008 and the present, the deployment of improved imaging technology on the recent set of lunar spacecraft generated a wealth of new high resolution imagery, and, assuming the accuracy of automatic CDA counting can be improved, the new high resolution images create an opportunity to characterize lunar crater production curves for very small diameter craters ( $5\text{m} \geq D < 100\text{m}$ ) as distinguished from small craters ( $100\text{m} \geq D < 1\text{km}$ ) and large craters ( $D \geq 1\text{km}$ ) (Lončarić and Salamunićcar, 2008). For future work, we propose to support CDA development by identifying matched NAC images that are illuminated by high and low sun angles, and those overlap regions will be distributed to the astronomy software research community in order to aid development of the next generation of CDA software.

**Kurt A. Fisher: New Developments in Counting Very Small Lunar Craters**

## **2 Background**

### **2.1 Direct measurements of the small lunar impact flux**

The National Research Council set as a minor lunar research goal to improve estimates of the real time meteor lunar impact flux (National Research Council, 2007, p. 21). The research team most focused on this question is NASA's Meteoroid Environment Office. In order to characterize the impact flux, the Meteoroid Environment Office monitors lunar impacts by small Earth-based telescopic video monitoring, and between 2005 and 2010 the Office observed 108 lunar meteoroid impact flashes over 212 hours of continuous observation. They found that the average impactor's mass is 100 grams, and a typical impactor produces a crater 13.5m in diameter (Cooke et al., 2007; Suggs et al., 2007; Suggs, 2010). From those observations, Suggs estimates an average lunar meteoroid impact flux of  $1.34 \times 10^{-7} \text{ km}^{-2} \text{ hr}^{-1}$ , which is equivalent to  $1.17 \times 10^{-3} \text{ km}^{-2} \text{ yr}^{-1}$  (Suggs, 2010, unpublished). Oberst used another form of real time lunar impact observing – seismic monitoring from stations on the lunar surface. He extracted impact observations was a network of small seismic recording stations deployed at several Apollo landing sites (the Apollo Passive Seismic Experiment) between 1969 to 1977 (Oberst, 1989; Kawamura et al., 2011). From this real time monitoring data, Oberst estimated the positions of 91 lunar meteoroid impacts that generated craters between “a few and tens of meters,” but he did not estimate an average meteor flux rate. An alternative method to finding the lunar meteor flux through video or seismic real time impact monitoring is retrospective study of lunar impact craters through spatial frequency diagrams. Improved crater counting studies for very small, very young craters ( $5\text{m} \geq D < 100\text{m}$ ) might also provide an additional boundary constraint on the Meteoroid Office's preliminary estimate of the lunar impact flux.

### **2.2 Historical high resolution lunar imagery**

Three researchers from the Apollo era previously computed spatial frequency diagrams for very small craters using high-resolution images from Lunar Orbiter series of candidate Apollo landing sites and Ranger series impact film, but those prior studies were based on images illuminated by widely sun angles. Greeley & Gault precisely measured thousands of small craters between 2.5m-10.0 m in diameter, and from one 1964 Ranger 7 P-1 camera image taken seconds before Ranger's impact on Mare Cognitum, Brinkmann measured craters between one and 10m in diameter (Brinkmann, 1966; Greeley & Gault, 1970). Shoemaker measured the distribution of very small craters from Ranger images. Greeley & Gault's very small crater measurements were part of a larger Apollo era program, described in Gault (1970), and in that program, approximately 20 researchers cataloged the spatial frequency distribution of the crater diameters between 10m to 1000m for more than 1.3 million craters. The source of their data where high resolution images covering about  $60,000 \text{ km}^2$  of 30 regions on the lunar surface from Lunar Orbiter II, III and V. But in Greeley & Gault's study, for example, sun angle illuminations varied between 10 degrees to 36 degrees.

After being taken in 1967, highest resolution engineering records for Lunar Orbiter V were archived in an inaccessible analogue format, and those images have only recently become available. LOV automatically processed wet film images while in lunar orbit, and in a process analogous to a fax transmission, the satellite converted those images to an analogue signal for broadcast to Earth-based receivers. The archived tapes were recordings of those transmissions. After proposals for the LRO took shape in the early 2000s, the U.S. Geological Survey began recovery of high resolution LOV images (Weller et al., 2007). It was only as recently as 2009 that NASA re-released digitized versions of 1967 high resolution images that could be recovered (Gaddis et al., 2009); however, the coverage of the recovered images is severely limited (U.S. Geologic Survey, 2011), and the recovery process continues (Epps & Sandler, 2011). These historical, but newly re-released, LOV high-resolution images have a new use. LOV images can be combined with new NAC high

**Kurt A. Fisher: New Developments in Counting Very Small Lunar Craters**

resolution imagery to estimate the lunar impact flux between 1967 and 2009, free of the observational bias of real time Earth based video or lunar based seismic monitoring.

Because the new NAC images potentially provide a wider selection of images under different solar illumination angles, new crater counts from the new imagery might yield revised lunar production crater curves for the very small crater class.

**2.3 New high resolution NAC lunar imagery**

Although improved lunar crater production curves for very small craters ( $5\text{m} \geq D < 100\text{m}$ ) might provide an additional boundary constraint on the Meteoroid Office's preliminary estimate of the lunar impact flux, counting very small craters requires high resolution images, and satellites sent to the Moon since 2009 have returned a bonanza of such images. Resolutions achieved by instruments aboard recent lunar satellites that could contribute new very small crater measurements include the following: the LRO NAC, 0.5 to 1.5m/pixel that has resolved 3m-30m diameter craters (Beyer et al., 2011; Xiao & Strom, 2011); Kaguya Terrain Camera (TC), 10m/pixel that has resolved 50m craters (Xiao & Strom, 2011); LRO mini-RF receiver, 30m/pixel that has resolved 150m diameter craters (Bell et al., 2011); LRO Wide Angle Camera (WAC), 75m/pixel (Scholten et al., 2011); and Chandrayaan-1, 140m/pixel (Lončarić et al., 2011). Additionally, the LRO Lunar Orbiter Laser Altimeter (LOLA) provides highly accurate surface altitude measurements at 5m diameter spots spaced 25m apart (Mazarico et al., 2010). The high resolution of LRO's NAC images considerably improve on the 1984 Clementine mission's nominal resolution of 100m/pixel and crater diameters of 500m (Werner & Medvedev, 2010b) and the 1965-1967 Lunar Orbiter I-V series' resolutions of 60m/pixel for the entire lunar surface.

Figure 1 through Figure 6 show high resolution NAC images illuminated by low, mid and high sun angles. NAC images also provide a unique new method for improving crater counting: stereograms created from matched images of the same area taken during consecutive LRO orbits. On some consecutive LRO orbital passes separated by about 90 minutes, the NAC captured overlapping images of the same terrain but at a slightly different angle. Figure 4 shows the foreshortening resulting from imaging the same feature from different angles, illustrated by two NAC images of the Crater Ina D feature taken on two consecutive orbits. As discussed below, Stopar et al. demonstrated how to combine two such images to compute the depths, as well as the diameters, of craters. Figure 6 illustrates an NAC image (Figure 5) processed to emphasize bright-rayed, fresh craters.

Kurt A. Fisher: New Developments in Counting Very Small Lunar Craters

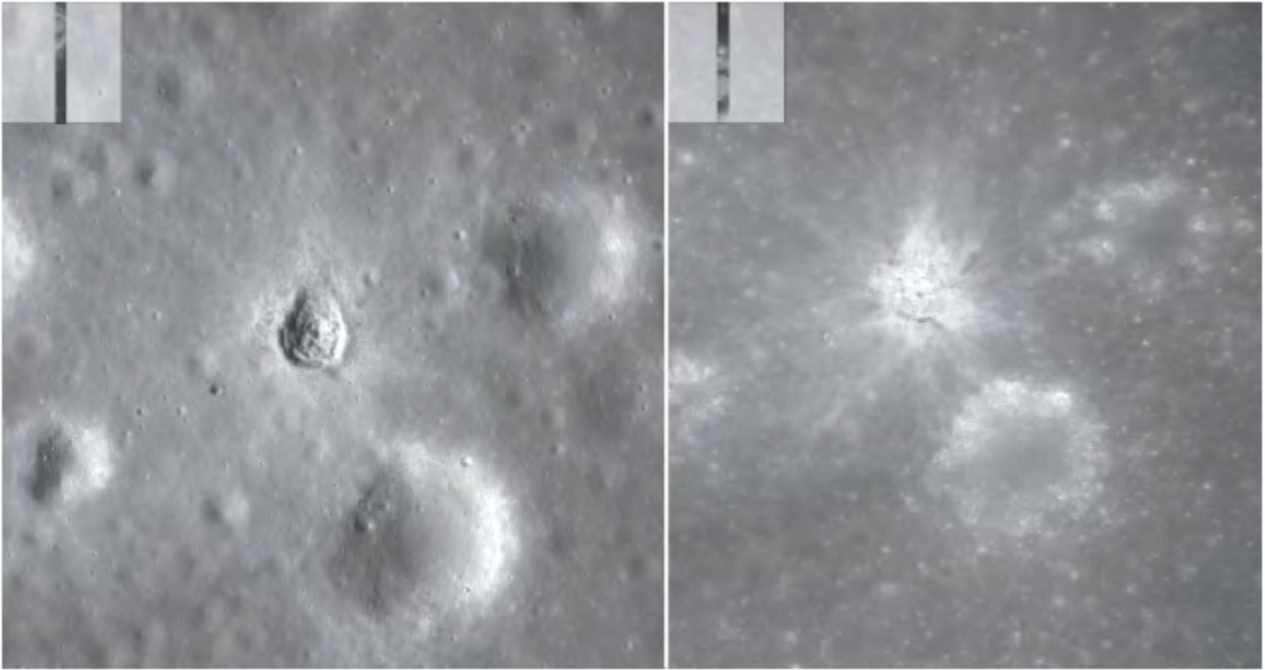


**Figure 1: ACT-REACT Map that excerpts from NAC images M104898806LE and M140291034LE north of Reiner Gamma near lunar coordinates N7.68, W49.53. The left image, M104898806LE, as taken under  $9.45^\circ$  solar illumination, and the right image, M140291034LE, was taken under  $48.08^\circ$  solar illumination. These images demonstrate how low angle illumination best captures crater rim details and how high angle illumination best highlights the ejecta patterns of bright-rayed young craters. A regional map showing the location of this crater is Figure 7, below. Credit: NASA/GSFC/Arizona State University/Applied Coherent Technology.**

Kurt A. Fisher: New Developments in Counting Very Small Lunar Craters

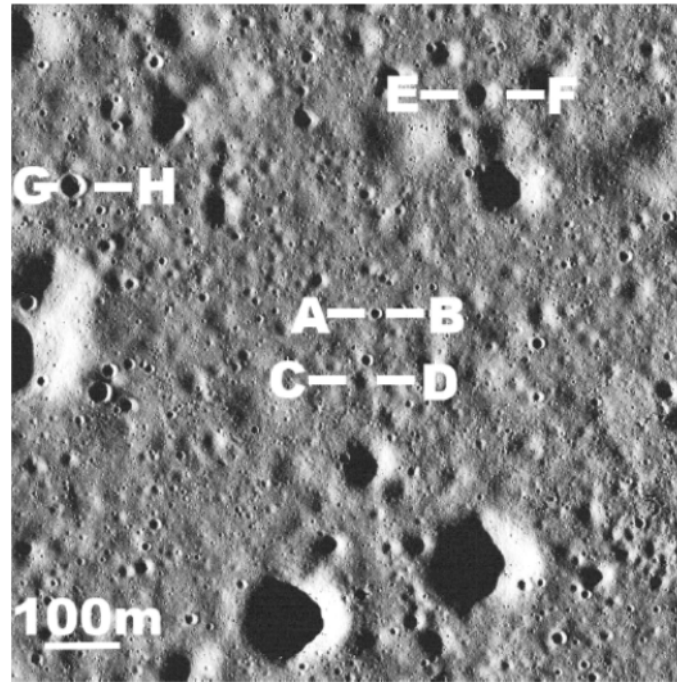


Figure 2: Low solar angle illumination image excerpted from an NAC image, M147454678LC, at Lines 1,500-3,499, Columns 1,939-2,266, near lunar coordinates N34.67, W72.53, under  $6.17^\circ$  solar illumination, but the image's brightness and contrast have been modified to enhance features. The white scale bar represents 100m, and the resolution of the original NAC image 0.72m/pixel. The image area covers  $1.74\text{km}^2$ , and it illustrates how low-angle illumination best captures crater rims. At higher display magnifications, small craters with fresh rims between 5m to 50m in diameter can be detected, but conversely, bright-rayed young craters are not highlighted as with high angle sunlight. Line segments A-B, C-D, E-F and G-H are discussed below. Credit: NASA/GSFC/Arizona State University.

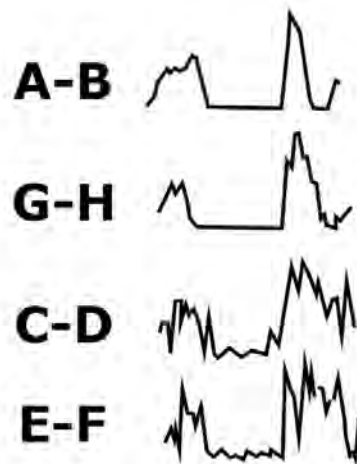
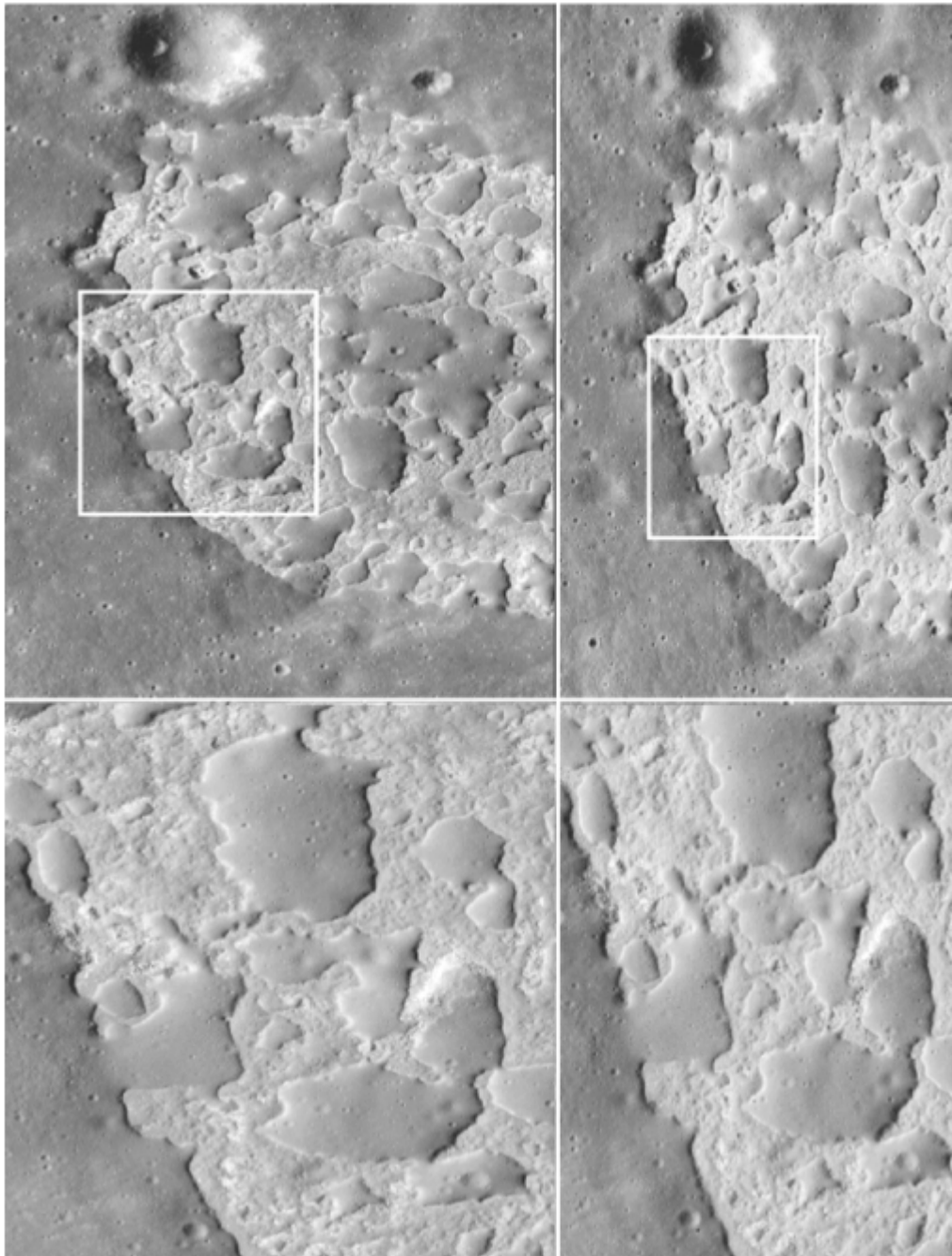


Figure 3: Raw image profiles of lines A-B, C-D and E-F marked on Figure 2. Line profiles also distinguish fresh and degraded crater rims.

Kurt A. Fisher: New Developments in Counting Very Small Lunar Craters



**Figure 4:** This montage of NAC images of C. Ina D taken on two successive orbits shows mid-range solar illumination (Left: M119808916LC, Right: M119815703LC near lunar coordinations N18.6, E5.3 under  $55\text{-}56^\circ$  solar illumination and with a difference in incidence angle of  $34.4^\circ$ .) These NAC images were identified in Stopar et al. (2010). The upper panels are wider angle views of these NAC images from ACT-REACT Map, and the white boxes in the upper panels denote regions covered by corresponding high resolution NAC image excerpts in the bottom panels. Each images' brightness and contrast have been modified to enhance features. The photographs illustrate how NAC images of the same feature taken from two successive LRO orbits can yield data from which stereograms might be constructed. Stopar et al. (2010) counted very small craters on the mare surface adjacent to C. Ina, and they estimated the craters' depths from stereograms constructed from images M119808916LC and M119815703LC. Credit: NASA/GSFC/Arizona State University.

Kurt A. Fisher: New Developments in Counting Very Small Lunar Craters

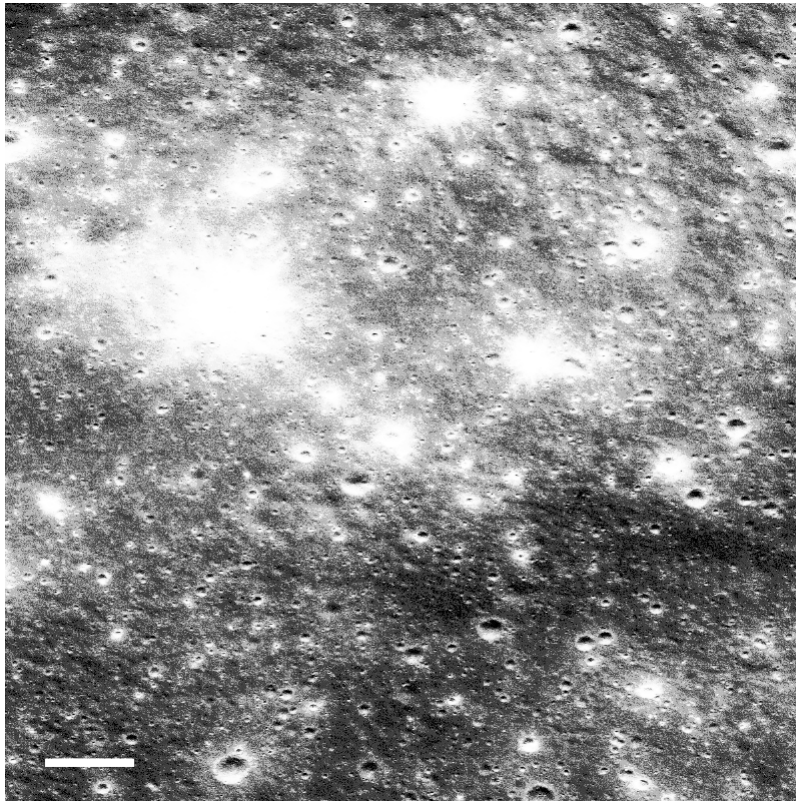


Figure 5: High solar angle illumination image excerpted from an NAC image, M155689122LE, at Lines 43,000-44,999, Columns 2,000-3,999, near lunar coordinates N31.21, W68.7, under  $60.2^\circ$  solar illumination, but the image's brightness and contrast have been modified to enhance features. The white scale bar represents 100m, and the resolution of the original image is 0.48m/pixel. The image size is approximately  $1.74\text{km}^2$ , and the photograph illustrates how high angle illumination emphasizes young fresh craters that are surrounded by bright rays. At higher display magnifications, bright ray craters between 5m to 50m in diameter can be detected, but conversely, the high angle of solar illumination washes out definition in the crater rims. Older very small craters with degraded rays and rims cannot be detected. Credit: NASA/GSFC/Arizona State University.

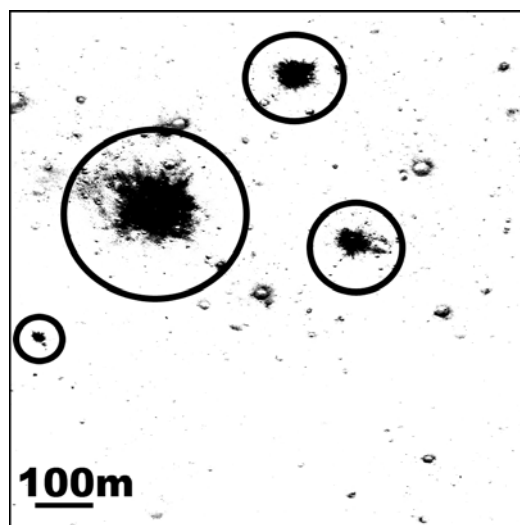
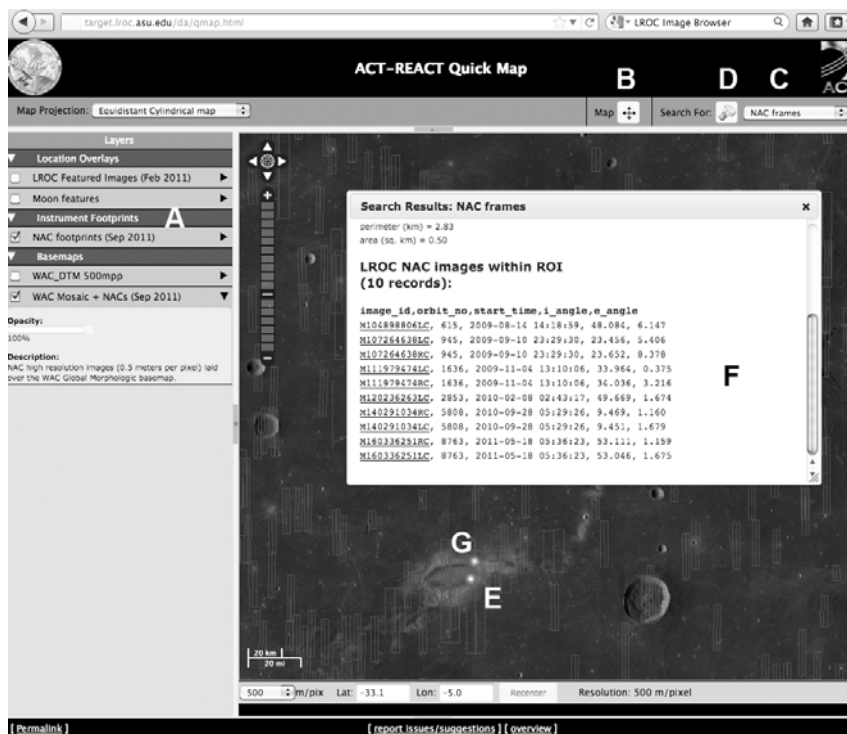


Figure 6: Same as Figure 5, but the high sun angle image is inverted and hypered. Now the bright-rayed fresh craters can be easily counted.

### Kurt A. Fisher: New Developments in Counting Very Small Lunar Craters

Another new technological development that aids very small crater counting is the Lunar Reconnaissance Orbiter Camera Team's (LROC) granting of easy, unrestricted internet access to the 503,206 LRO image archive, but image retrieval methods have limitations that prevent efficient identification of image overlaps by sun altitude angles. First, the LROC Image Browser allows retrieval of NAC images for a user-specified square region of the lunar surface by sun angle (NASA & School of Earth and Space Exploration, 2010), and second, NASA and the LROC Team also provide a web applet, named the "ACT-REACT Map," that conversely allows for the visual spotting of overlapping high resolution images. Neither retrieval application supports efficient filtering to only retrieve images that overlap at user selected high and low sun angle images (NASA & School of Earth and Space Exploration, 2011). Figure 7 shows an illustrative ACT-REACT Map screenshot. Other NAC image portals include the Lunar Orbital Data Explorer (NASA & Washington University at St. Louis, 2010) and NASA LRO PDS Image Node (NASA et al., 2011).



**Figure 7: Example screenshot from the LROC Team's ACT-REACT Map at selenographic coordinates latitude N7.68, longitude W58.63. The graphic illustrates the ACT-REACT Map application's ability to and limitations of rendering overlapping NAC images of differing sun angle elevations. Annotations on the graphic show key points on the use of the ACT-REACT Map applet. Point A: Activate display of the boundaries of NAC images on the search map. Point B: Set mode to pan map. Point C: Set to retrieve information on NAC images. Point D: Set mode to retrieve information on NAC images at the next click point. Point E: Clicking on the ACT-REACT base map near Reiner Gamma feature to retrieve data on available NAC images at that point. Point F: Retrieval screen data returned by the ACT-REACT applet. Point G: Point near Reiner Gamma shown in Figure 1, above. This ACT-REACT Map screenshot shows that there are numerous potential image overlap areas, but it is inefficient to manually review each potential overlap region in order to determine if a high-low illumination match exists. Credit: NASA/GSFC/Arizona State University/Applied Coherent Technology.**

Figure 7 also demonstrates an anecdotal limitation seen in high resolution NAC images. Overlap of available high and low sun angle images tends to occur in small areas at the north or south ends of each image, and thus the number of the highest quality data regions suitable for CDA testing purposes may be low and are difficult to identify. Currently, the ACT-REACT public applet appears

**Kurt A. Fisher: New Developments in Counting Very Small Lunar Craters**

to contain NAC images limited to the LROC Team's 7th Release; the applet does not contain NAC images from the first through fifth releases. Nonetheless, individual images can be easily retrieved from the LROC Team's archive, and the availability of these images have high resolution images have reinvigorated CDA research.

**2.4 New developments in automatic counting of very small lunar craters**

Inspired by this new wealth of easily accessible high resolution LRO NAC images, researchers are developing new techniques to support the next generation of CDA crater counting and digital elevation terrain mapping (DEM) software, and these new techniques can improve CDA counting of very small lunar craters ( $5\text{m} \geq D < 100\text{m}$ ). Salamunićar & Lončarić (2008) list 68 prior CDA articles concerning the Moon and Mars that were published between 2000 and 2007, and twenty-five of those articles were published between 2005 and 2007. Bandeira et al. (2010) notes that these earlier CDAs were developed to detect large craters on low resolution images and that those algorithms are inefficient at detecting small craters on high resolution images, but the next generation of CDA software could be extended to counting very small craters with a diameter less than 100m.

Several examples of small crater counting techniques were published during 2010-2011. Stopar et al. used stereograms from two NAC high resolution images to reconstruct the profiles of 85 bright-rayed craters between 40m to 200m in diameter near C. Ina (Stopar et al., 2010). Scholten et al. combined LRO LOLA and LRO WAC imagery into a global lunar digital elevation map (DEM) with a resolution of 200m/pixel, and from those images, their automated crater counting method resolved craters that are "tens of meters in diameter" (Scholten et al., 2010). Using three NAC images and a crater counting module available for the commercial ArcGis software, Hiesinger et al. compared crater counts for small craters between 10-300m in diameter in young melt pools on the floor of C. Copernicus with areas in Copernicus's ejecta rays, and they conclude that the younger melt pools were aged between 113M and 237M years (Hiesinger et al., 2010b). Morita et al. experimented using Fourier transforms to count craters on simulated images and DEMs (Morita et al., 2010). In other software advances, the U.S. Geological Survey developed and released a large crater count analysis plugin and a crater measuring helper plugin for use with the ArcGis product (U.S. Geologic Survey, 2010). Lončarić et al. applied shape-from-shading (SfS) computation techniques to Chandrayaan-1 imagery to construct a digital elevation map (DEM), and they then automatically counted 33% craters (N=125 of 387) in lunar test regions (Lončarić et al., 2011). Their crater detection resolution limit based on 140m/pixel Chandrayaan images was  $1/512^\circ$  or about 60m. In comparison, Bandeira et al. created a CDA that accurately detected 83% of small craters larger than 200m in diameter from high resolution surface images of Mars (Bandeira et al., 2010), and Grumpe & Wöhler successfully demonstrated the accuracy of the SfS DEM technique on lunar surfaces of varying albedo (Grumpe & Wöhler, 2011). Several research groups in the United States and Europe are independently testing experimental DEM software against two agreed LRO NAC lunar images (Beyer et al., 2011), and of those groups, Beyer et al. combined SfS DEMs made from the NAC test images and LOLA elevation data.

**2.5 New developments in manual counting of very small lunar craters**

Prior to the digital age, manual techniques were used to count craters, but even manual counting techniques benefit from computer-aided processing. In the 1970s, Greeley & Gault used teams of up to 8 graduate students to count 333,404 small craters, and for quality control, Greeley & Gault both limited counters to two-hour shifts and followed counters by deviation from the mean analysis in order to exclude inaccurate counts (Greeley & Gault, 1970). Greeley & Gault recommended crater counting by groups of counters, not individual counters, in order to control for observer counting bias, and even with good controls, his crater counter measurements still varied by 20% around the

**Kurt A. Fisher: New Developments in Counting Very Small Lunar Craters**

mean. Since 2009, Moon Zoo Project have been combining Internet distributed computing with general public volunteers to classify and count 5,043,360 lunar features, including very small craters, over a seven month period (Citizens Science Alliance & Moon Zoo Team, 2011; Gay et al., 2011). One advantage of the Moon Zoo Project's approach is that deviation from the mean analysis can be used to detect and to adjust for such counting biases by well-known methods. Researchers with the Moon Zoo Project propose to use distributed volunteer counting for very small craters using NAC images (Joy et al., 2011; Lintott, 2010), but the Project began in mid-2010 and results are still forthcoming.

Recently, other researchers have applied traditional manual crater counting techniques to count very small diameter craters from LRO NAC images. Using high resolution LRO NAC images of a small region near C. Alphonsus, Xiao & Strom measured craters down to 3m in diameter from NAC images, but they do not state the total surface area from which they extracted their counts (Xiao & Strom, 2011). They also used lower resolution Kaguya images to measure larger craters in the same region, and in order to study the effect of solar illumination angle on crater counts, Ostrach et al. used high resolution NAC images of a region northeast of C. Lambert to report crater counts down to 50m in diameter (Ostrach et al., 2011). Ostrach et al. recorded crater counts for craters down to 10m in diameter, but they declined to utilize crater counts for craters with a diameter below 50m due to concerns over the resolution limit of NAC images biasing their tallies. Bouley & Baratoux measured 662 craters on one NAC image with diameters between 65m and 1000m, while using the slope of those craters in order to test whether slope is an indicator of crater degradation and age, and they found a consistent pattern in the slope of degraded craters within crater diameter classes between 90m and 360m (Bouley & Baratoux, 2011). Robinson et al. used crater counting of very small craters between 3m and 50m to relatively date the elevated butte and depressed valley regions within the Ina D feature (Robinson et al., 2010) (*see* Figure 4). While manual crater counting remains the best method for obtaining statistically valid count results, manual counting is labor intensive and less cost efficient than automated counting.

**3 New controversies concerning counting very small craters ( $5m \geq D < 100m$ )**

The future of very small crater counting remains with automated counting techniques, assuming that count accuracy of CDAs can be increased. Other researchers call into question whether very small crater counting is intrinsically flawed, and they question whether the any counting technique can ever yield statistically valid lunar crater production curves.

**3.1 Variation in very small crater counts caused by surface geology**

One researcher asserts that lunar crater production curves can never be produced from the new NAC images of very small craters. Xiao & Strom raise questions concerning whether crater counting of very small and small craters can produce statistically valid lunar crater production curves based on impact variations caused by surface geology (Xiao & Strom, 2011). Based on crater counts extracted from LRO and Kaguya images of C. Alphonsus (that resolve very small craters (3m-30m dia.) and small craters (50-1000m)), Xiao & Strom (2011) concluded that such crater counts are dominated by secondary impacts and that the number of preserved craters varies by the nature of geologic surface materials. Xiao & Strom's conclusion regarding secondary impact contamination of very small crater counts reaches an incorrect conclusion because they did not comply with generally accepted crater reporting methodology by reporting the size of area that they surveyed. Crater Analysis Techniques Working Group et al.'s standard methodology requires enumerating the key metric of the surface area examined (Crater Analysis Techniques Working Group et al., 1979). Since only a small number of fresh craters can be expected to be found within the few square kilometers covered by a single high resolution image, the variation in spatial frequency counts that Xiao & Strom found may be the result of sampling too small a surface area.

**Kurt A. Fisher: New Developments in Counting Very Small Lunar Craters**

In contrast, Ostrach et al. qualifies their conclusions on sun angle illumination contamination of small craters counts due to their small 4km<sup>2</sup> survey area, that “may be too small to adequately assess the small crater population” (*id.*).

**3.2 Variation in very small crater counts caused by sun angle illumination**

Another researcher feels valid crater counting might be prevented by variations between images of sun angle illumination. Ostrach et al. compared very small craters down to 10m in diameter on Apollo Metric and NAC high resolution images that were illuminated by the different local sun angles, and they concluded that the number of craters that could be counted varied significantly by the angle of solar illumination (Ostrach et al., 2011). Ostrach et al. also note that this is not a new finding. As early as 1975, Young suggested that sun angle can be compensated for computationally (Young, 1975), and modern SFD and antapex-apex modeling compensates for both latitudinal and longitudinal variations by computational adjustments (Le Feuvre & Wieczorek, 2011; Gallant et al., 2009).

**3.3 Contamination of very small crater counts by secondary impacts**

Due to secondary impact contamination, some researchers object to the use of larger crater SFDs and Neukum’s Production Function (NPF) to date solar system surfaces with respect to small craters (McEwen, 2003, 2006; Wells et al., 2010), or they restrict their crater count analysis to craters larger than 20km in diameter to avoid count contamination from secondary impacts (Marchi & Bottke, 2010). (Neukum’s NPF is the generally accepted standard that estimates the number of craters by class on a one-giga year nearside lunar mare surface. For those unfamiliar with the NPF, Section 1 of the Appendix provides a background on the function and explains how the NPF is used to relatively date lunar surfaces.) Wells et al. demonstrated contamination of crater counts on the floors of C. Newton and Newton-A from secondary impacts craters with a diameter between 400m-2km, where the secondary impacts originated from Tycho (Wells et al., 2010). Conversely, Head et al. found no significant secondary crater effect for craters larger than 20km based on a global analysis of highland and maria craters (Head et al., 2010).

Neukum’s rebuttal to the secondary impact criticism is that Malin et al.’s recent observation of fresh impact craters on Mars illustrates that the NPF for Mars adequately incorporates the secondary impact effect (Neukum, 2008; Malin et al., 2006). Using Malin’s data for Martian craters with a diameter of 20m-100m, Neukum plotted a SFD, and he concluded that the spatial frequency slope for Malin’s fresh craters nearly matched the slope of the Martian NPF (Neukum, 2008). All of these objections to study of the spatial frequency of very small craters can be resolved, and those objections should not present only a caution, and not a barrier, to reinvigorated crater counting efforts.

**4 Paths to resolving new controversies for counting very small craters**

The secondary impact contamination objection can be avoided by counting only bright, fresh, young craters and by careful control of distance to nearby craters greater than 100m in diameter. Misinterpretations concerning secondary impact contamination can be avoided by adoption of a lunar planetary community consensus on the minimum survey size for very small craters from which valid statistical results can be obtained. Better archive image retrieval tools would allow researchers to gather a sufficient number of samples of similarly sun illuminated images in order to conduct statistically valid studies.

**Kurt A. Fisher: New Developments in Counting Very Small Lunar Craters**

#### **4.1 Discussion of the secondary impact contamination objection**

The secondary impact contamination objection warrants a preliminary analysis response, if further studies of the lunar production function for very small craters can be justified. There are several reasons why secondary impact contamination may not significantly contaminate crater counts for very small craters ( $5\text{m} \geq D < 100\text{m}$ ) as opposed to small and large craters ( $100\text{m} \geq D \leq 100\text{km}$ ).

Recent objections by researchers to surface dating by SFDs based on secondary impact contamination originate from Soderblom's 1970 modeling of surface erosion from very small crater impacts (Soderblom, 1970). From high-velocity gun experiments on a simulated lunar surface, Gault found that as new impacts accumulate on a sand surface, any new impacts eventually erase an existing craters (Gault, 1970; Soderblom, 1970). The point at which any incremental crater must erode an existing crater is the saturation point, and Soderblom also modeled that over time the impacted surface reaches an equilibrium of newly created and destroyed surfaces. The experimentally observed erosion of craters is caused by secondary contamination from the ejecta from new strikes. Soderblom's modeling also suggests a spatial frequency diagram slope near -3.8. Very small lunar crater counting by Shoemaker and Brinkmann, based on spatial frequency diagrams computed from Ranger images, found crater frequency slopes between -3.3 and -4.0 for craters smaller than 1km (Soderblom, 1970), which was in the range predicted by Soderblom. Soderblom's experimental SFD slope near -3.8 is also consistent with Neukum et al.'s lunar crater production function. Of particular concern to very small crater counting is that a crater may not originate from a unique impact; a very small crater have been caused by a boulder secondarily ejected from a nearby large impact.

Other research suggests that secondaries from nearby large craters may not be expected to contaminate very small crater spatial frequency counts due to surface re-gardening, saturation equilibrium and rapid small crater ray degradation. In the 1970s, Gault used high-velocity gun experiments to characterize the regolith gardening process, and in 1974, Gault et al. modeled the probability that any one square kilometer of the lunar surface would be overturned by direct or nearby impacts to a specified depth (Gault et al., 1974). Using Monte Carlo techniques, Gault et al. estimated that the top 1cm of lunar soil is turned over between 1,000 and 10,000 times over a 10,000,000 year period, and other stochastic modeling suggests that any single point on the lunar surface may be raising from a baseline to 30cm in height and excavated in depth 10cm below the baseline on a timescale of 24 million years (Heiken et al., 1991, p. 89).

Closely related to repeated surface turnover is equilibrium saturation, and Neukum's production function also incorporates the concept of equilibrium saturation. The NPF supports the proposition that for small craters under 100m in diameter, each kilometer of lunar surface is re-gardened over geologically relatively small time periods. Gault and Soderblom showed that for very small craters, as impacts accumulate on a surface over time, a saturation point is quickly reached in which any new impact will degrade an adjacent crater.

Kurt A. Fisher: New Developments in Counting Very Small Lunar Craters

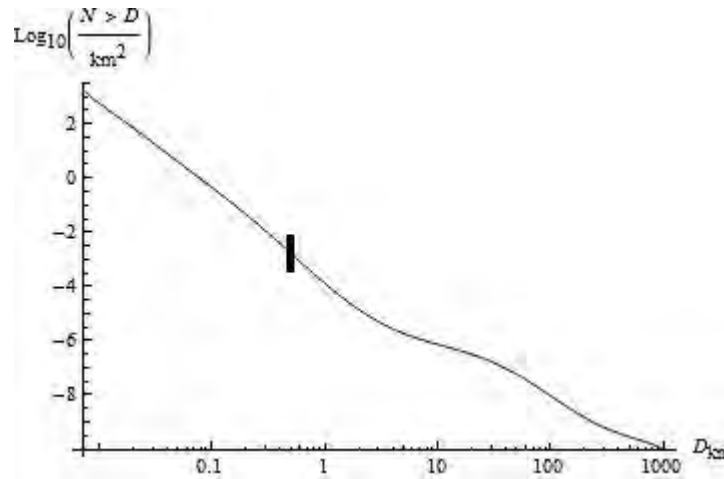


**Figure 8: Plot of the Neukum lunar crater production curve (Neukum et al., 2001). The function models the log base 10 of the number of cumulative craters larger than the chosen crater diameter D within one square kilometer and aged less than 1 Ga years. For the smallest crater within the function’s domain, 10m, the function predicts there will be 102.78 craters larger than 10m (N=602) in any one square kilometer on the lunar surface. The thick bar represents the approximate cross-over point. To the left of the cross-over point, the lunar surface is constantly resurfaced, or “gardened,” by numerous small impacts. To the left of the cross-over point, a historical record of impact craters is not preserved due to this constant resurfacing. To the right of the cross-over point, the lunar surface records an unchanged historical collection of large crater impacts over the last one billion years.**

Neukum’s twelve term logarithmic lunar production function (Appendix Eq. 3, Figure 8) can be integrated with respect to time to yield a chronology function in the general form of Eq. 1 (Neukum et al., 2001; Neukum, 2011). Equation 2 is Neukum’s chronology function integrated from App. Eq. 3 for 1km craters, and Figure 9 plots the 1km diameter crater chronology function over 3.5 giga years.

$$N(D, t) = (A \times (e^{Bt} - 1)) + (Ct) ; \text{ for } D \text{ km craters across time } t. \tag{1}$$

$$N(1) = (5.44 \times 10^{-14} \times (e^{6.93t} - 1)) + (8.38 \times 10^{-4} \times t) ; \text{ for } 1\text{km craters across time } t. \tag{2}$$

## Kurt A. Fisher: New Developments in Counting Very Small Lunar Craters

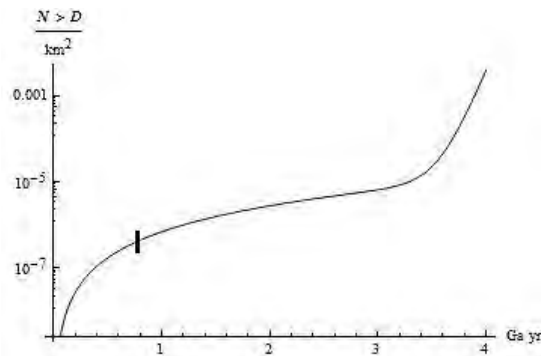


**Figure 9: Plot of the Neukum crater chronology function for craters with 1km in diameter after Eq. 2 (Neukum et al., 2001). The chronology function models the number of cumulative craters larger than the chosen crater diameter as a function of time for a period between 0 and 1 giga year. The bar approximates the saturation equilibrium point for 1km craters. After the saturation point is reached, new 1m diameter craters erase older 1km diameter craters, and the rate of accumulation slows. For 1km craters, saturation equilibrium is reached before 1 giga year. For very smaller diameter craters, saturation equilibrium will be reached earlier than 1 giga year, and for larger craters, for example 10km and above, saturation equilibrium is not reached within the known age of the Moon. A separate chronology function exists for any given crater diameter class within the valid domain of the Neukum production function, as discussed in the main text.**

As Figure 9 illustrates, a square kilometer of lunar surface quickly saturates within the first billion years of impacts, that is the surface reaches saturation equilibrium. After saturation, new 1km craters created between 1 to 3 giga years will not appreciably change the appearance of the lunar surface. For small craters less than 100m in diameter, the equilibrium saturation point will be reached far earlier than 1 giga year, and this process in part explains Hiesinger et al.'s earliest dating of Tycho melt pool surfaces by crater counting at 113M years. Extrapolating these results for Neukum's chronology function to the limits of Neukum's production function at 0.01km diameter craters suggests that the saturation equilibrium point for small and very small craters occurs over a relatively short geologic time period.

This extrapolation is supported by Ivanov's dating of very small craters between 10m and 100m in diameter at four locations by associating craters with surface ages estimated by cosmic ray exposure (Ivanov, 2006). Ivanov counted very small craters around craters from which Apollo missions returned surface rocks. Once the lunar rocks were returned to Earth, the rocks could be dated from measurements of the degree of surface degradation that they exhibited caused by cosmic rays (*id*). Ivanov concluded for very small craters that the age of gardened mare surfaces was at most 100M years old, and he speculated that for very small craters, the best working estimate of secondary contamination of counts is 25% to 50% of the total and is not the higher estimate of  $\geq 75\%$  secondary contamination made by others. Ivanov suggests exercising caution in reaching conclusions until more small crater SFDs can be obtained from new high resolution imagery and until those small craters are ground truthed by dating rocks returned to Earth by future lunar missions.

That the lunar surface is turned over rapidly by very small impacts is also suggested by a higher rate of bright ray degradation within progressively smaller crater diameter classes. While a given square kilometer of lunar surface might contain an older 1m diameter secondary impact crater, for example an impact that occurred 750M years ago from C. Tycho, a very small crater is more likely to be degraded within the last 1 million years from numerous small impacts. For 400m-100km diameter craters, gardening does not have the same proportional effect on bright lunar rays as the gardening of very small craters between 5m-100m in diameter. The turnover of the top 1cm of ejecta from a

**Kurt A. Fisher: New Developments in Counting Very Small Lunar Craters**

50km crater may not dim that impact's thick bright ray, while the same surface turnover for a thin bright ray layer surrounding a 10m diameter crater might be erased. Although the period over which ray degradation occurs for very small craters is not well understood, recent results by Suzuki et al. and Werner & Medvedev suggest that for craters larger than 300m, the duration of bright-ray retention decreases with crater diameter (Suzuki et al., 2010; Werner & Medvedev, 2010a).

Even if some secondary impact contamination occurs from nearby 100m impacts, such secondaries can be more easily excluded from crater counts. Since 1m ejecta would not be expected to travel significant distances from a lower energy 100m impact, associations between and exclusions of 1m-5m diameter secondaries from 100m bright rayed impact craters could be identified and excluded from very small crater counts. In contrast, a large Tycho class impact makes many 1km-20km secondaries that travel large distances across the Moon's surface. Additionally, for very small craters below 100m in diameter, photographic resolution may self-limit secondary impact contamination when counting such craters. For a large impact, like the 86km diameter C. Tycho, ejecta created many secondaries 1km in diameter. A hypothetical similarly scaled 50m small impact crater might create many one-half meter secondaries, but those secondaries are below the crater resolution limit of NAC images.

Robinson et al. is illustrative of misinterpretations that can arise from applying the NPF and Neukum's chronology function to very small craters below the saturation equilibrium point (Robinson et al., 2010). Because a high number of 5m-50m craters ( $N > 3000$ ) were found in their counts of small areas on the valleys and buttes of the Ina D feature, Robinson et al. relied on Neukum et al.'s NPF and concluded that Ina D was more than 1 giga year old. However, as Robinson et al. acknowledges, their conclusions are at odds with six other prior researchers who found that the Ina D feature is young. Because Robinson et al. counted very small craters that are below the equilibrium saturation point for very small craters, a small region can have a density of craters near the boundary limit of the NPF curve and still be young due to constant re-gardening by more frequent, very small impacts. As the diameter of an impact crater decreases, the time to equilibrium saturation decreases (Fig. 9). The NPF for very small craters extracted from high resolution images will have the densities modeled by Neukum et al. for surfaces aged 1 giga year, but those densities do not mean that those surfaces are 1 giga year old at very small diameters. For very small craters to the left of the equilibrium point (Fig. 9), the surface may have been gardened more than once, and thus, the actual surface age is younger even though the apparent age derived from crater counting is older.

**4.2 Establish a consensus on survey region size by crater diameter**

Since there may only be one or two bright-rayed very-small craters in any given square kilometer of the lunar surface, large areas of the lunar surface must be surveyed in order to characterize the spatial frequency distribution of very small craters. As Gault noted for the Apollo era, researchers surveyed 60,000km<sup>2</sup> in order to produce a SFD for both rayed and non-rayed craters with diameters between 10m-1000m. While Crater Analysis Techniques Working Group et al. established standards for the display of crater counts, they did not specify minimum survey region sizes that would be required to produce statistically valid crater counts for each class of crater diameters. In light of the controversies described above regarding small crater counting, Crater Analysis Techniques Working Group et al. (1979) should be revisited on this point.

**4.3 Improve tools to identify image overlaps by sun angle illumination**

Crater counts do vary significantly by sun angle illumination, but the half-million LROC image archive and improved retrieval indexing would allow researchers to gather sufficient numbers of images of a similar illumination to conduct new research. The highest-quality studies the could be

**Kurt A. Fisher: New Developments in Counting Very Small Lunar Craters**

done by counting very small craters using new high resolution imagery would match images from four sources. First, historical high-solar illumination Lunar Orbiter V images for 36 limited areas of the nearside surface can be matched with low solar illumination NAC images. Once registered, such matched images would allow CDA software to match bright-rayed very small craters on high solar illumination images with very small craters that show younger well defined rims on low illumination images. Second, historical high-solar illumination LOV high resolution images could be matched with current high solar illumination NAC images. After registration and image difference processing, it would be possible to detect very-small bright-rayed crater impacts that occurred between the taking of LOV images in 1967 and the taking of NAC images during 2009-2010. An example that illustrates the viability of the historical comparison technique is NASA's 2010 detection of a new 10m diameter lunar crater that was formed between 1971 and 2009. NASA compared an old Apollo 15 high resolution image with a modern NAC image to detect the new crater (Daubar, 2010). Similarly, in 2006, Malin et al. detected 20 new impact craters that had diameters between 2m-150m and that formed on Mars between 1999 and 2006 by comparing old and more recent Mars Global Surveyor images (Malin et al., 2006). Third, NAC low and high solar illumination images could be matched for overlap. Fourth, stereograms from images made on successive orbits provide additional data on crater depth.

However, the LROC Image Browser (NASA & School of Earth and Space Exploration, 2010), the ACT-REACT Map applet (NASA & School of Earth and Space Exploration, 2011), the NASA Lunar Data Explorer (NASA & Washington University at St. Louis, 2010), and the NASA LRO PDS Image Node NASA et al. (2011) do not support efficient identification of overlapping NAC images for a user requested location by classes of solar illumination, and the ACT-REACT Map applet currently does not provide coverage of all LROC images. The LROC Image Browser does allow filtering of NAC images by orbit number, box region and sun angle, and therefore the browser can be used to identify stereogram candidates. Proposed future work will address these cross-referencing barriers to new CDA research.

**5 Future work and conclusion**

For future work, overlapping NAC images will be identified on nearside lunar maria where one image was taken under high solar illumination and where the second image was taken under low solar illumination. The source images will be the 503,206 LRO images released by the LROC Team through September 2011, Release No. 7. The image cross-reference list will provide a set of test image areas consistent with (Salamunićar & Lončarić's process for improving CDAs (Salamunićar & Lončarić, 2008). A second list cross-referencing overlaps between historical LOV high resolution high sun angle images and existing low-illumination NAC images will also be prepared. Such cross-reference lists, when coupled with LRO laser altimeter data on surface roughness and Clementine multi-spectral images on surface composition, will aid developers of improved CDA software in improving the accuracy of their automated counting of very small lunar craters ( $5\text{m} \geq D < 100\text{m}$ ). A lunar production curve for very small lunar craters could provide an upper boundary constraint for estimates of the current lunar meteor impact flux. The development of improved CDA software is a prerequisite to further investigation of the spatial frequency distribution of very small craters using high resolution NAC images, where automated counting has a low accuracy rate. Manual crater counting through Internet distributed volunteers is an alternative to automated counting by CDA software. Improved CDA and counting software will have application on other solar system bodies. A follow up article will illustrate the use of NASA PDS Viewer to extract subparts from NAC images and how to locate candidate NAC images using the LRO Image Browser and ACT-REACT Map.

**Kurt A. Fisher: New Developments in Counting Very Small Lunar Craters****References**

- Bandeira, L., Ding, W., & Stepinski, T. F. (2010). Automatic detection of sub-km craters using shape and texture information. In: *41st Lunar and Planetary Science Conference, held March 1-5, 2010 at The Woodlands, Texas*. Woodlands, Texas: Lunar Planetary Inst., Abs. 1144.
- Bell, S. W., Thomson, B. J., Dyar, M.D., & Bussey, D.B.J. (2011). Dating fresh lunar craters with mini-RF. In: *42nd Lunar and Planetary Science Conference, held March 7-11, 2011 at The Woodlands, Texas*. Woodlands, Texas: Lunar Planetary Inst., Abs. 342.
- Beyer, R. et al. (2011). LROC DTM comparison. In: *42nd Lunar and Planetary Science Conference, held March 7-11, 2011 at the Woodlands, Texas*. Woodlands, Texas: Lunar Planetary Inst., Abs. 2715.
- Bouley, S. & Baratoux, D. (2011). Variation of small crater degradation on the Moon. In: *42nd Lunar and Planetary Science Conference, held March 7-11, 2011 at The Woodlands*. Woodlands, Texas: Lunar Planetary Inst., Abs. 1388.
- Brinkmann, R. T. (1966). Lunar crater distribution from the Ranger 7 photographs. *J. Geophys. Res.*, 71, pp. 340-342.
- Citizens Science Alliance Moon Zoo Team (2011). *Moon Zoo (Webpage)*. <http://www.moonzoo.org/> Last accessed 5 Nov. 2011.
- Cooke, W. J., Suggs, R. M., Suggs, R. J., Swift, W. R., & Hollon, N. P. (2007). Rate and distribution of kilogram lunar impactors. In: *38th Lunar and Planetary Science Conference, held March 12-16, 2007 in League City, Texas*. League City, Texas: Lunar Planetary Inst., Abs. 1986.
- Crater Analysis Techniques Working Group et al. (1979). Standard techniques for presentation and analysis of crater size-frequency data. *Icarus*, 37(2), pp. 467-474, doi:10.1016/0019-1035(79)90009-5 .
- Daubar, I. (2010, Jul. 27). *New Impact Crater on the Moon! (Press Release)*. url: <http://lroc.sese.asu.edu/news/?archives/260-New-Impact-Crater-on-the-Moon!.html>. Last accessed 1 Nov. 2011.
- Epps, A. D. & Sandler, M. (2011). Recovering Lunar Orbiter framelets from digitized magnetic tape record. In: *42nd Lunar and Planetary Science Conference, held March 7-11, 2011 at The Woodlands, Texas*. Woodlands, Texas: Lunar Planetary Inst., Abs. 2416.
- Gaddis, L., Becker, T., Weller, L., Hare, T., & Isbell, C. (2009). Lunar Orbiter digital frame mosaics: Ready for prime time. In: *40th Lunar and Planetary Science Conference, held March 23-27, 2009 at The Woodlands, Texas*. Woodlands, Texas: Lunar Planetary Inst., Abs. 2437.
- Gallant, J., Gladman, B., & Cuk, M. (2009). Current bombardment of the Earth-Moon system: emphasis on cratering asymmetries. *Icarus*, 202(2), pp. 371-382, doi:10.1016/j.icarus.2009.03.025.
- Gault, D.E., 1970. Saturation and equilibrium conditions for impact cratering on the lunar surface: criteria and implications. *Radio Science*, 5, pp. 273-291, doi:10.1029/RS005i002p00273.

**Kurt A. Fisher: New Developments in Counting Very Small Lunar Craters**

Gault, D. E., Hoertz, F., Brownlee, D. E., & Hartung, J. B. (1974). Mixing of the lunar regolith. In: *Proceedings of the 5th Lunar Science Conference, held March 18-22, 1974 in Houston, Texas*. New York City: Pergamon Press. Vol. 3, pp. 2365-2386.

Gay, P. L., Cormier, S., Brown, S., Huang, D., Prather, E., Brissenden, G., Daus, C., & Moon Zoo Team (2011). Moon Zoo: Engaging the public in geomorphology, learning, and community. In: *42nd Lunar and Planetary Science Conference, held March 7-11, 2011 at The Woodlands, Texas*. Woodlands, Texas: Lunar Planetary Inst., Abs. 1701.

Greeley, R. & Gault, D. E. (1970). Precision size-frequency distributions of craters for 12 selected areas of the lunar surface. *The Moon*, 2(1), pp. 10-77, doi:10.1007/BF00561875.

Grumpe, A. & Wöhler, C. (2011). A photometric approach to the construction of lunar digital elevation maps using Chandrayaan-1 M3 imagery in combination with laser altimetry data. In: *42nd Lunar and Planetary Science Conference, held March 7-11, 2011 at The Woodlands, Texas*. Woodlands, Texas: Lunar Planetary Inst., Abs. 1478.

Hartmann, O. & Neukum, G. (2010). Impact-Chronology Model as mass-estimate method for impacted masses on planetary surfaces. In: *41st Lunar and Planetary Science Conference, held March 1-5, 2010 at The Woodlands, Texas*. Woodlands, Texas: Lunar Planetary Inst., Abs. 2082.

Head, J. W., Fassett, C. I., Kadish, S. J., Smith, D. E., Zuber, M. T., Neumann, G. A., & Mazarico, E. (2010). Global distribution of large lunar craters: Implications for resurfacing and impactor populations. *Science*, 329, pp. 1504-1507, doi:10.1126/science.1195050.

Heiken, G. H., Vaniman, D. T., & French, B. M. (1991). *A Lunar Sourcebook - A User's Guide to the Moon*. Cambridge, England: Cambridge Univ. Press.

Hiesinger, H. (2003). Ages and stratigraphy of mare basalts in Oceanus Procellarum, Mare Nubium, Mare Cognitum, and Mare Insularum. *J. Geophys. Res.*, 108(E7), 5065, doi:10.1029/2002JE001985.

Hiesinger, H., Head, J. W., Wolf, U., Jaumann, R., & Neukum, G. (2010a). Ages and stratigraphy of lunar mare basalts in Mare Frigoris and other nearside maria based on crater size-frequency distribution measurements. *J. Geophys. Res.*, 115, E03003, doi:10.1029/2009JE003380.

Hiesinger, H. & Head, J. W. I. (2006). New views of lunar geoscience: An introduction and overview. *Reviews in Mineralogy and Geochemistry*, 60(1), pp. 1-81, doi:10.2138/rmg.2006.60.1.

Hiesinger, H., van Der Bogert, C. H., Pasckert, J. H., Robinson, M. S., Klemm, K., Reiss, D., & LROC Team (2010). New crater size-frequency distribution measurements for Copernicus Crater based on Lunar Reconnaissance Orbiter camera images. In: *41st Lunar and Planetary Science Conference, held March 1-5, 2010 at The Woodlands, Texas*. Woodlands, Texas: Lunar Planetary Inst., Abs. 2304.

Huang, J., Xiao, L., Yang, J., & Dong, Y. S. (2010). New model ages of mare material in Sinus Iridum, Moon. In: *41st Lunar and Planetary Science Conference, held March 1-5, 2010 at the Woodlands, Texas*. Woodlands, Texas: Lunar Planetary Inst., Abs. 1184.

**Kurt A. Fisher: New Developments in Counting Very Small Lunar Craters**

Ivanov, B. A. (2006). Earth/Moon impact rate comparison: Searching constraints for lunar secondary / primary cratering proportion. *Icarus*, 183(2), pp. 504-507, doi: 10.1016/j.icarus. 2006. 04.004.

Joy, K., Crawford, I., and Grindrod, P. et al. (2011). Moon Zoo: citizen science in lunar exploration. *Astronomy and Geophysics*, 52(2), 20000-20002.

Kawamura, T., Morota, T., Kobayashi, N., & Tanaka, S. (2011). Cratering asymmetry on the Moon: New insight from the Apollo Passive Seismic Experiment. *Geophys. Res. Ltr.*, 381, L15201, doi:10.1029/2011GL048047.

Le Feuvre, M. & Wieczorek, M. A. (2011). Nonuniform cratering of the Moon and a revised crater chronology of the inner Solar System. *Icarus*, 214, pp. 1-20, doi:10.1016/j.icarus.2011.03.010.

Lintott, C. (2010). Moon Zoo: First science results. In: *European Planetary Science Congress 2010 held Sept. 19-24, 2010 at the Pontifical Univ. of Saint Thomas Aquinas, Rome, Italy*. PlanetEuro Res. Infrastructure, Toulouse Cedex, France. Abs. No. 900.

Lončarić, S., Salamunićcar, G., Grumpe, A. & Wöhler, C. (2011). Automatic detection of lunar craters based on topography reconstruction from Chandrayaan-1 M3 imagery. In: *42nd Lunar and Planetary Science Conference, held March 7-11, 2011 at The Woodlands, Texas*. Woodlands, Texas: Lunar Planetary Inst., Abs. 1454.

Malin, M.C., Edgett, K.S., Posiolova, L.V., McColley, S.M. & Dobra, E.Z.N. (2006). Present-day impact cratering rate and contemporary gully activity on Mars. *Science*, 314, pp. 1573-1577, doi:10.1126/science.1135156.

Marchi, S., Mottola, S., Cremonese, G., Massironi, M., & Martellato, E. L. (2009). A new chronology for the Moon and Mercury. *Astron. J.*, 137(6), 4936-4948, doi:10.1088/0004-6256/137/6/4936.

Mazarico, E., Watters, W. A., Barnouin, O. S., Neumann, G. A., Zuber, M. T., Smith, D. E., & LOLA Science Team (2010). Depth-diameter ratios of small craters from LOLA multi-beam laser altimeter data. In: *41st Lunar and Planetary Science Conference, held March 1-5, 2010 at the Woodlands, Texas*. Woodlands, Texas: Lunar Planetary Inst., Abs. 2443.

McEwen, A. S. (2003). Secondary cratering on Mars: Implications for age dating and surface properties. In: *Sixth International Conference on Mars, held July 20-25, 2003 in Pasadena, California*. Houston, Texas: Lunar Planetary Inst., Abs. 3268.

McEwen, A. S. (2006). Cratering age considerations for young terranes in the inner Solar System. In: *Workshop on Surface Ages and Histories: Issues in Planetary Chronology, held May 23-23, 2006, Houston, Texas*. Houston, Texas: Lunar Planetary Inst., Abs. 6030.

Michael, G. G. & Neukum, G. (2010). Planetary surface dating from crater size-frequency distribution measurements: Partial resurfacing events and statistical age uncertainty. *Earth & Planetary Sci. Ltr.*, 294, pp. 223-229, doi:10.1016/j.epsl.2009.12.041.

**Kurt A. Fisher: New Developments in Counting Very Small Lunar Craters**

Morita, S., Asada, N., Demura, H., Hirata, N., Terazono, J., Ogawa, Y., Honda, C., & Kitazato, K. (2010). Approach to crater chronology with Fourier transform of digital terrain model. In: *41st Lunar and Planetary Science Conference, held March 1-5, 2010 at The Woodlands, Texas*. Woodlands, Texas: Lunar Planetary Inst., Abs. 1990.

NASA School of Earth & Space Exploration, Ariz. St. Univ. (2010). *LROC WMS Image Browser (Web application)*. url: <http://wms.lroc.asu.edu/lroc>. Last accessed 1 Nov. 2011.

NASA & School of Earth & Space Exploration, Ariz. St. Univ. (2011). *LROC ACT-REACT Quick Map (Web application)*. url: <http://target.lroc.asu.edu/da/qmap.html>. Last accessed 1 Nov. 2011.

NASA, U.S. Geologic Survey, & Jet Prop. Lab. (2011). *PDS Imaging Note: Lunar Reconnaissance Orbiter Online Data Volumes (Web page)*. url: <http://pds-imaging.jpl.nasa.gov/volumes/lro.html>. Last accessed 3 Nov. 2011.

NASA & Washington Univ. at St. Louis (2010). *Lunar Orbital Data Explorer*. url: <http://odestage.rsl.wustl.edu/moon/>. Last accessed 3 Nov. 2011.

National Research Council (2007). *The Scientific Context for Exploration of the Moon: Final Report*. Washington, D.C.: National Academies Press.

Neukum, G. (1982). *Meteoritenbombardement und Datierung Planetarer Oberflächen*. Dissertation, Ludwig-Maximilians-University of Munich.

Neukum, G. (2008). The lunar and martian cratering records and chronologies. In: *39th Lunar and Planetary Science Conference, held March 10-14, 2008 in League City, Texas*. League City, Texas: Lunar Planetary Inst., Abs. 2509.

Neukum, G. (2011). *Craterstats (Software)*. url: <http://hrscview.fu-berlin.de/craterstats.html> Last accessed 1 Nov. 2011.

Neukum, G., Ivanov, B. A., & Hartmann, W. K. (2001). Cratering records in the inner Solar System in relation to the Lunar Reference System. *Space Sci. Rev.*, 96, pp. 55-86, doi:10.1023/A:1011989004263.

Oberst, P. J. (1989). *Meteoroids near the Earth-Moon System as inferred from temporal and spatial distribution of impacts detected by the Lunar Seismic Network*. Ph.D. Thesis, The Univ. of Texas at Austin, Texas.

Ostrach, L. R., Robinson, M. S., Denevi, B. W., & Thomas, P. C. (2011). Effects of incidence angle on crater counting observations. In: *42nd Lunar and Planetary Science Conference, held March 7-11, 2011 at The Woodlands, Texas*. Woodlands, Texas: Lunar Planetary Inst., Abs. 1202.

Pike, R. J. (1974). Depth-diameter relations of fresh lunar craters - Revision from spacecraft data. *Geophys. Res. Ltr.*, 1, pp. 291-294, doi:10.1029/GL001i007p00291.

Robinson, M. S., Thomas, P. C., Braden, S. E., Lawrence, S. J., Garry, W. B., & LROC Team (2010). High resolution imaging of Ina: Morphology, relative ages, formation. In: *41st Lunar and Planetary Science Conference, held March 1-5, 2010 at The Woodland, Texas*. Woodland, Texas: Lunar Planetary Inst., Abs. 2592.

**Kurt A. Fisher: New Developments in Counting Very Small Lunar Craters**

Salamunićcar, G. and Lončarić, S. (2008). Open framework for objective evaluation of crater detection algorithms with first test-field subsystem based on MOLA data. *Adv. in Space Res.*, 42, pp. 6-19, doi:10.1016/j.asr.2007.04.028.

Scholten, F. and Oberst, J. and Matz, K.D. and Roatsch, T. and Wahlisch, M., Robinson, M.S. & LROC Team (2011). GLD100 -The Global Lunar 100 Meter Raster DTM from LROC WAC stereo models. In: 42nd Lunar and Planetary Science Conference, held March 7-11, 2011 at The Woodlands, Texas. Woodlands, Texas: Lunar Planetary Inst., Abs. 2046.

Scholten, F., Oberst, J., & Robinson, M. S. (2010). Multi-Scale lunar impact crater topography from LROC WAC/NAC stereo Data. In: *Nördlingen Ries Crater Workshop, held June 25-27, 2010 in Nördlingen, Germany*. Houston, Texas: Lunar Planetary Inst., Contribution No. 7041.

Shoemaker, E. M. (1965). Preliminary analysis of the fine structure of the lunar surface in Mare Cognitum. In J. Hess, D. H. Menzel (ed.), *The Nature of the Lunar Surface*, pp. 23+.

Shoemaker, E. M., Hait, M. H., Swann, G. A., Schleicher, D. L., Dahlem, D. H., Schaber, G. G., & Sutton, R. L. (1970). Lunar regolith at Tranquility Base. *Science*, 167, pp. 452-455, doi:10.1029/JB075i014p02655.

Soderblom, L. A. (1970). A model for small-impact erosion applied to the lunar surface. *J. Geophys. Res.*, 75(14), pp. 2655-2661, doi:10.1029/JB075i014p02655.

Stöffler, D., Ryder, G., Ivanov, B. A., Artemieva, N. A., Cintala, M. J., & Grieve, R. A. F. (2006). Cratering History and Lunar Chronology. *Reviews in Mineralogy and Geochemistry*, 60(1), 519-596, doi:10.2138/rmg.2006.60.05.

Stopar, J. D., Robinson, M., Barnouin, O. S., & Tran, T. (2010). Depths, diameters, and profiles of small lunar craters from LROC NAC stereo images. In: *Proceedings of the American Geophysical Union, Fall Meeting 2010, held Dec. 13-17, 2010 in San Francisco, Calif.* Washington, D.C.: AGU, Abs. # P53C-1543AGU. Available at url: <http://adsabs.harvard.edu/abs/2010AGUFM.P53C1543S>. Last accessed 1 Nov. 2011.

Suggs, R. M. (2010, May 12). *Lunar Meteoroid Impact Observations and the Flux of Kilogram-sized Meteoroids (Slide Presentation)*. NASA Meteoroid Environ. Office. Available from url: [http://ntrs.nasa.gov/archive/nasa/casi.ntrs.nasa.gov/20100023306\\_2010023834.pdf](http://ntrs.nasa.gov/archive/nasa/casi.ntrs.nasa.gov/20100023306_2010023834.pdf). Last accessed 1 Nov. 2011.

Suggs, R. M., Cooke, W. J., Suggs, R. J., Swift, W. R., & Hollon, N. P. (2007). The NASA Lunar Impact Monitoring Program. *Earth, Moon, and Planets*, 102(1-4), 293298.

Suzuki, S., Honda, C., Hirata, N., Asada, N., Demura, H., Kitazato, K., Ogawa, Y., Terazono, J., Moroda, T., Ohtake, M., Haruyama, J., & Matsunaga, T. (2010). Retention time of rays around small lunar craters. In: *Proceedings of the American Geophysical Union, Fall Meeting 2010, held Dec. 13-17, 2010 in San Francisco, Calif.* Washington, D.C.: AGU, Abs. # P53C-536AGU. Available at url: <http://adsabs.harvard.edu/abs/2010AGUFM.P53C1536S>. Last accessed 1 Nov. 2011.

U.S. Geologic Survey (2010). *GIS Tools and Scripts (Webpage)*. Available at url: <http://webgis.wr.usgs.gov/pigwad/tutorials/scripts/index.html>. Last accessed 1 Nov. 2011.

**Kurt A. Fisher: New Developments in Counting Very Small Lunar Craters**

Weller, L., Becker, T., Archinal, B., Bennett, A., Cook, D., Gaddis, L., Galuszka, D., Kirk, R., Redding, B., & Soltesz, D. (2007). USGS Lunar Orbiter Digitization Project: Updates and status. In: *38th Lunar and Planetary Science Conference, held March 12-16, 2007 in League City, Texas*. League City, Texas: Lunar Planetary Inst., Abs. 2092.

Wells, K. S., Campbell, D. B., Campbell, B. A., & Carter, L. M. (2010). Detection of small lunar secondary craters in circular polarization ratio radar images. *J. Geophys. Res.*, 115, E06008, doi:10.1029/2009JE003491.

Werner, S. C., Harris, A. W., Neukum, G., & Ivanov, B. A. (2002). The Near-Earth Asteroid size-frequency distribution: A snapshot of the lunar impactor size-frequency distribution. *Icarus*, 156(1), pp. 287-290, doi:10.1006/icar.2001.6789.

Werner, S. C. & Medvedev, S. (2010a). Lunar rayed craters. In: *41st Lunar and Planetary Science Conference, held March 1-5, 2010 at The Woodlands, Texas*. Woodlands, Texas: Lunar Planetary Inst., Abs. 1058.

Werner, S. C. & Medvedev, S. (2010b). The Lunar rayed-crater population: Characteristics of the spatial distribution and ray retention. *Earth & Planetary Sci. Ltr.*, 295(1-2), 147-158, doi:10.1016/j.epsl.2010.03.036.

Xiao, Z. & Strom, R. G. (2011). Problem in crater counting by small craters - peeking at the geologic history of Crater Alphonsus. In: *42nd Lunar and Planetary Science Conference, held March 7-11, 2011 at the Woodlands, Texas*. Woodlands, Texas: Lunar Planetary Inst., Abs. 2046.

Young, R.A., 1975. Mare crater size-frequency distributions: Implications for relative surface ages and regolith development. In: *6th Lunar Science Conference, held March 17-21, 1975 at Houston Texas*. Houston, Texas: Lunar Planetary Inst., pp. 2645-2662.

## 6 Appendix

### 6.1 Background on the Neukum Lunar Crater Production Function (NPF)

Neukum’s lunar crater production function (NPF) is a twelve term logarithmic differential equation (App. Eq. 3) that estimates the density of craters by diameter per each square kilometer on nearside lunar surface (Neukum, 1982; Neukum et al., 2001; Michael & Neukum, 2010). Figure 8 is a plot of Neukum’s NPF. Neukum developed the function for large craters by counting only fresh, bright-rayed craters with diameters greater than 250m with an estimated age of less than one giga year on lunar mares. The NPF is meant to estimate the total craters aged less than one giga year that would expected be to counted in any single square kilometer, and notwithstanding whether a crater is young, bright-rayed or not. For very small craters under 100m in diameter, Neukum used crater counts made by Shoemaker et al. from Apollo 11 and 12 landing sites to establish the upper boundary condition of the NPF (Ivanov, 2006), and Neukum asserts the function is valid down to craters of 10m in diameter (Neukum et al., 2001; Neukum, 2011).

$$\begin{aligned}
 \log_{10} N(D) = & -3.876 + (-3.557528(\log_{10} D)^1) \\
 & + (0.781027(\log_{10} D)^2) + (1.021521(\log_{10} D)^3) \\
 & + (-0.156012(\log_{10} D)^4) + (-0.444058(\log_{10} D)^5) \\
 & + (0.019977(\log_{10} D)^6) + (0.086850(\log_{10} D)^7) \\
 & + (-0.005874(\log_{10} D)^8) + (-0.006809(\log_{10} D)^9) \\
 & + (0.000825(\log_{10} D)^{10}) + (0.0000554(\log_{10} D)^{11}).
 \end{aligned}
 \tag{3}$$

The NPF represents the logarithm of the cumulative number of craters larger than a specific class. Table 1 shows a hypothetical simple crater count made from an image illustrates the how the raw count of craters relates to the logarithm of the cumulative number of craters larger than a specific class. This method of tabulating craters was pioneered by Baldwin and was refined by the Crater Analysis Working Group (Baldwin, 1964; Crater Analysis Working Group, 1978).

Crater dia. cohort	Raw count	Cumulative count	Cumulative class	Cumulative count>	Log Cumulative >
0m -99m	1000	1000	≤100m	1111	3
100m - 999 m	100	1100	>100m	111	2
1km – 9.9km	10	1110	>1km	10	1
10km – 100km	1	1111	>10km	1	0

**Table 1 – Hypothetical crater count by raw and cumulative crater diameter cohort. The log slope of the rightmost column is approximately -1.**

The NPF’s valid domain is ambiguously reported in literature. Neukum et al. (2001) state that the 2001 updated NPF is valid from 100m to 200km, but the function datafile that supports Neukum’s Craterstats software in Neukum (2011), also citing Neukum et al. (2001), states that the NPF is valid from 10m to 100km. For this paper, the NPF is assumed to be valid between 10m and 100km.

**Kurt A. Fisher: New Developments in Counting Very Small Lunar Craters**

Other publications misreport the  $a_0$  coefficient of twelve-term logarithmic NPF as -3.0876 (Neukum et al., 2001; Stöffler et al., 2006; Hiesinger et al., 2010a). The  $a_0$  coefficient used in Neukum's CraterStats software is -3.876 (Neukum, 2011), and that coefficient correctly replicates Neukum's prior published plots of the NPF in Neukum et al. (2001) and in Stöffler et al. (2006). For computations in this paper, the NPF  $a_0$  coefficient is assumed to be -3.876, because that coefficient is used by Neukum in his most recent version of CraterStats.

Spatial frequency diagrams (SFDs) can be used to relatively date surfaces, as shown in Figure 10. Surfaces younger than the calibrated NPF curve are shifted to the left, and older surfaces are shifted to the right of the calibration curve.

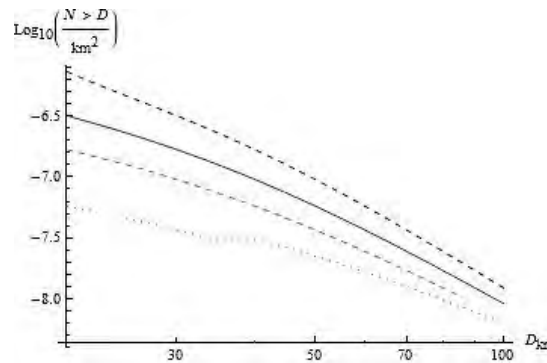


**Figure 10: Neukum's calibrated lunar production curve for larger craters over the last 1 Ga years is used to relatively date surfaces on other Solar System bodies. Neukum's calibrated production curve (Figure 8) is the solid center curve for craters with diameters between 15km-100km. The left-lower dashed curve represents a crater counts from a hypothetical surface on a Solar System body. That surface is younger than the calibrated lunar surface because the surface has experienced fewer cumulative impacts than the calibrated lunar surface. The right-upper dashed curve represents a crater counts from a hypothetical surface on a Solar System body that is older than the calibrated lunar surface. The surface has experienced more cumulative impacts as compared to the calibrated lunar surface. The left lower dotted curve represents a surface that experienced a resurfacing event that erased part of the crater record. The horizontal line portion of the curve is the resurfacing event.**

SFDs made from crater counts can be paired with radiometric dating of surface samples returned by Apollo missions and with Clementine reflectance remote sensing that allows for extrapolation of surface compositions to large areas on the Moon, and combining those data types creates a robust chronological dating model for the mare surface of the Moon (e.g. Hiesinger (2003); Hiesinger & Head (2006)). Recent examples of combining crater counts with reflectance remote sensing include Head et al. (2010), Hiesinger et al. (2010a), and Huang et al. (2010). The similarity of the SFD of crater diameters in the NPF to the presumed source of objects that create craters - the Asteroid Belt -also supports the validity of the NPF model (Werner et al., 2002; Hartmann & Neukum, 2010), and Marchi et al. proposed a new model that replicates the SFD of the NPF by modeling from the distribution of asteroid diameters to lunar mare SFDs for impactors between 0.1m and 72km in size (Marchi et al., 2009).